Particulates Vs fibers: Dimension featured magnetic and visible light driven photocatalytic properties of Sc modified multiferroic bismuth ferrite nanostructures

M. Sakar,[a] S. Balakumar,[a,*] P. Saravanan,[b] S. Bharathkumar,[a]

[a,]National Centre for Nanoscience and Nanotechnology, University of Madras, Guindy campus, Chennai 600025, India. *E-mail: balasuga@yahoo.com.*
[b]Defence Metallurgical Research Laboratory, Hyderabad 500058, India.

Electronic Supplementary Information

S1. Morphology analysis

The formation kinetics of the cubic like morphology of Bi1-xScxFeO3 particulate compositions is depicted in Fig. S1. It is known that the selective binding habit of surfactants on a particular crystallographic facet decides the size and shape of the crystals.[31] It is reported that the citric acid (CA) possesses the habit of binding on <111> surface and allows the <100> surface to grow.[32] The insert of Fig. S1 illustrates the crystallographic surface of a cubic shape.[33] Accordingly, in our system, the subsequent nucleation and growth of the particles further assisted by the CA by means of its selective binding on <111> surface. This binding process essentially restricted the growth of <111> surface and allowed the <100> surface to grow and led to the cubic morphology. It is also reported that the CA has threshold to bind the surface of the particles.[34] Despite the size and shape of the particles controlled by CA, their aggregated nature might have resulted from subsiding of threshold energy compared to the thermodynamics of nanoparticles aggregation.

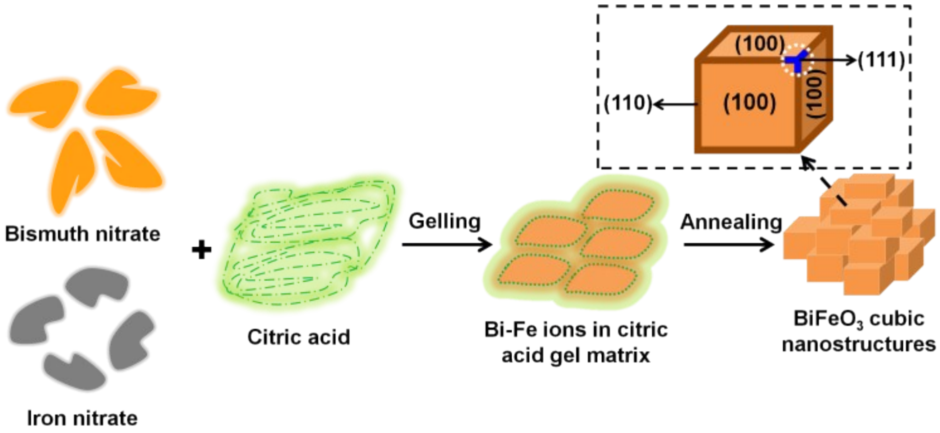

Fig. S1 Formation of cube like morphology of $BiFeO_3$ nanostructures. (Insert image shows the crystallographic surface in a cubic system)

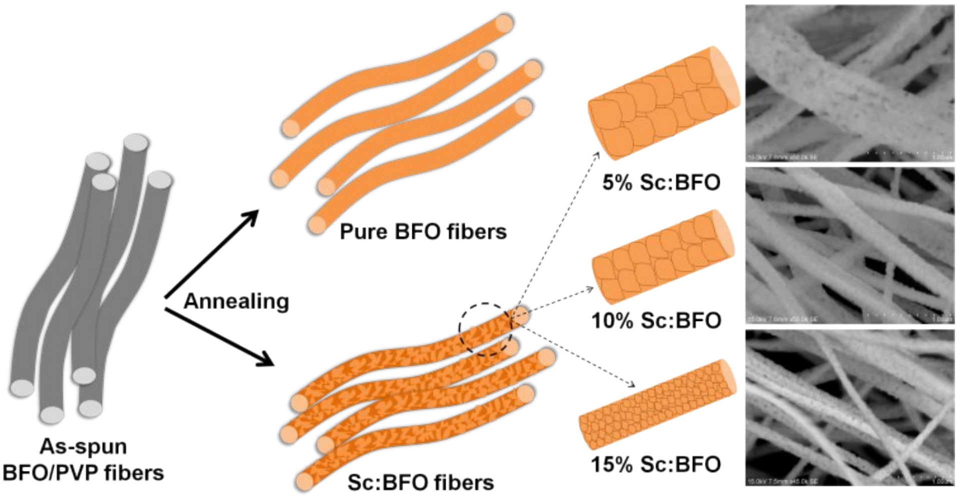

Fig. S2 Formation of $Bi_{1-x}Sc_xFeO_3$, (where $x = 0.05, 0.1, 0.15$) fiber nanostructures.

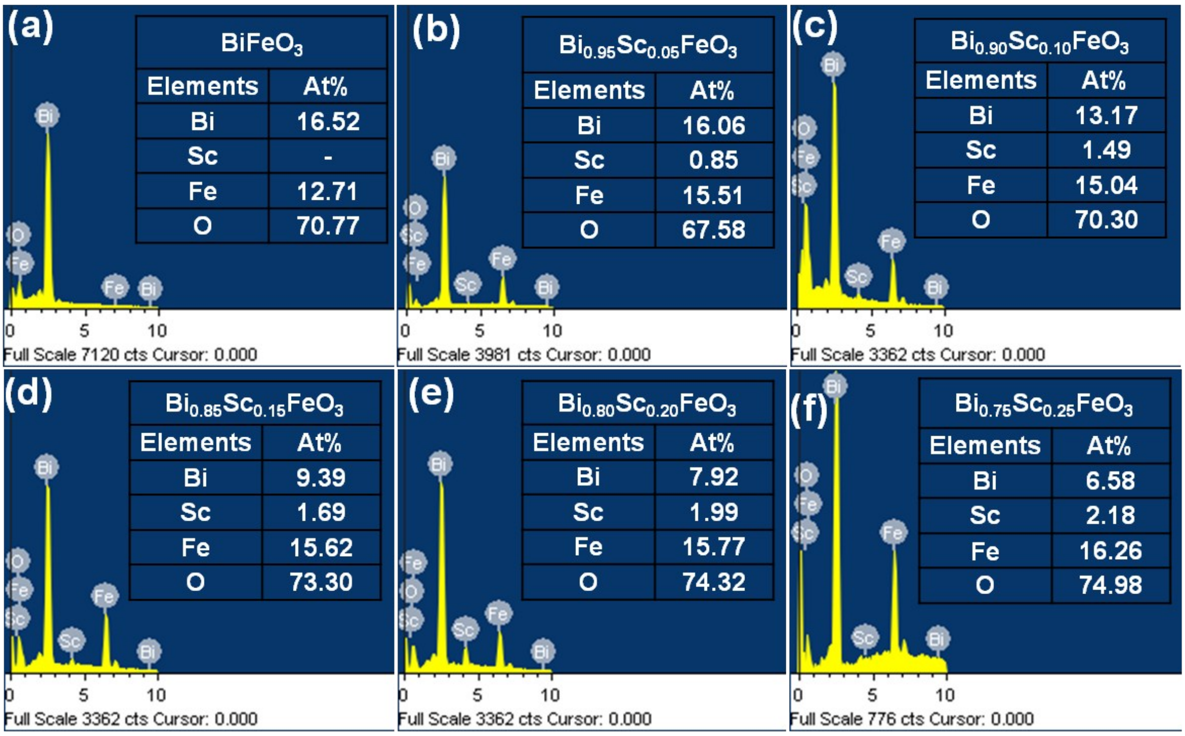

(a) $BiFeO_3$

Elements	At%
Bi	16.52
Sc	-
Fe	12.71
O	70.77

(b) $Bi_{0.95}Sc_{0.05}FeO_3$

Elements	At%
Bi	16.06
Sc	0.85
Fe	15.51
O	67.58

(c) $Bi_{0.90}Sc_{0.10}FeO_3$

Elements	At%
Bi	13.17
Sc	1.49
Fe	15.04
O	70.30

(d) $Bi_{0.85}Sc_{0.15}FeO_3$

Elements	At%
Bi	9.39
Sc	1.69
Fe	15.62
O	73.30

(e) $Bi_{0.80}Sc_{0.20}FeO_3$

Elements	At%
Bi	7.92
Sc	1.99
Fe	15.77
O	74.32

(f) $Bi_{0.75}Sc_{0.25}FeO_3$

Elements	At%
Bi	6.58
Sc	2.18
Fe	16.26
O	74.98

Fig. S3 Energy dispersive X-ray spectra of $Bi_{1-x}Sc_xFeO_3$, particulate nanostructures where x = (a) 0.0, (b) 0.05, (c) 0.10, (d) 0.15, (e) 0.20 and (f) 0.25.

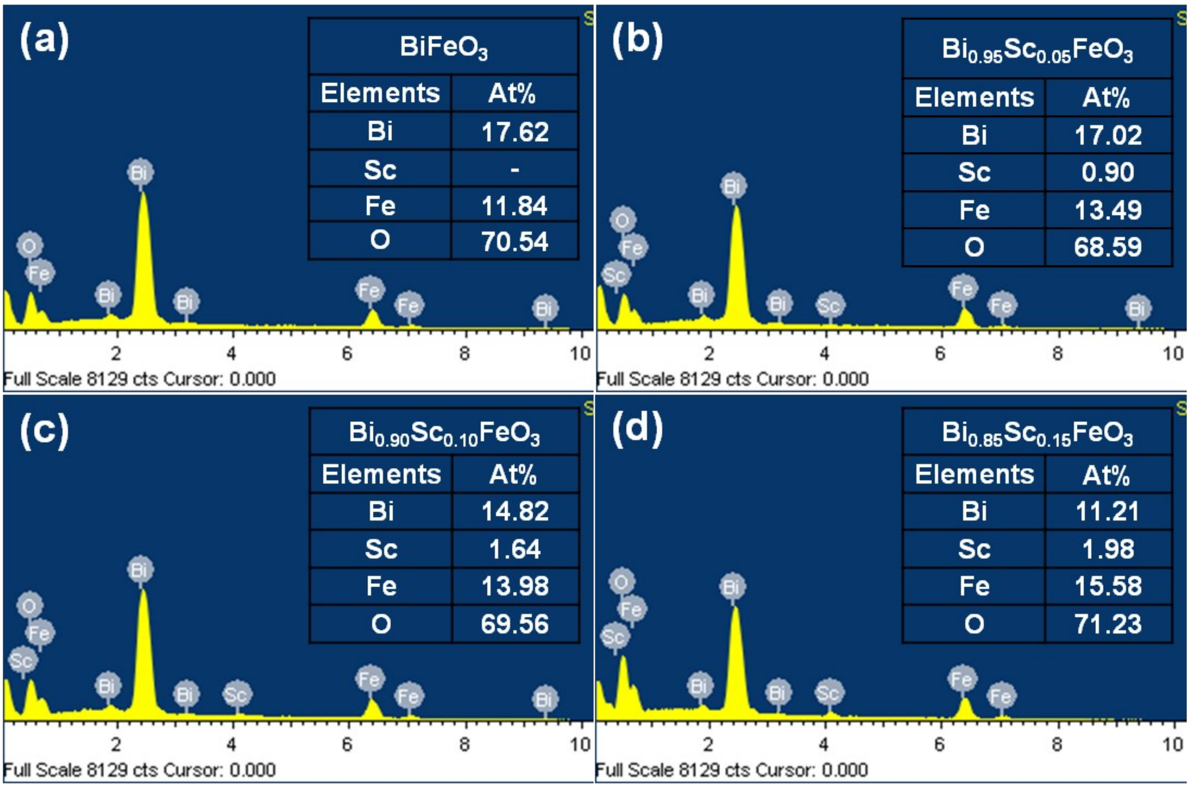

(a) $BiFeO_3$

Elements	At%
Bi	17.62
Sc	-
Fe	11.84
O	70.54

(b) $Bi_{0.95}Sc_{0.05}FeO_3$

Elements	At%
Bi	17.02
Sc	0.90
Fe	13.49
O	68.59

(c) $Bi_{0.90}Sc_{0.10}FeO_3$

Elements	At%
Bi	14.82
Sc	1.64
Fe	13.98
O	69.56

(d) $Bi_{0.85}Sc_{0.15}FeO_3$

Elements	At%
Bi	11.21
Sc	1.98
Fe	15.58
O	71.23

Fig. S4 Energy dispersive X-ray spectra of $Bi_{(1-x)}Sc_{(x)}FeO_3$, fiber nanostructures, where x = (a) 0.0, (b) 0.05, (c) 0.10, and (d) 0.15.

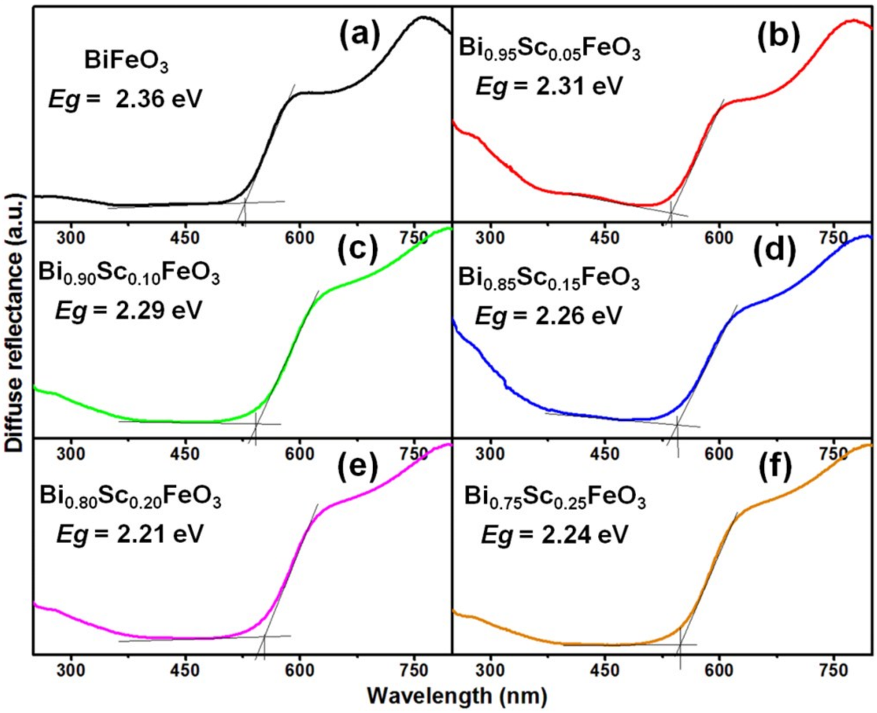

Fig. S5 Diffuse reflectance spectrum of $Bi_{1-x}Sc_xFeO_3$, particulate nanostructures, where x = (a) 0.0, (b) 0.05, (c) 0.10, (d) 0.15, (e) 0.20 and (f) 0.25.

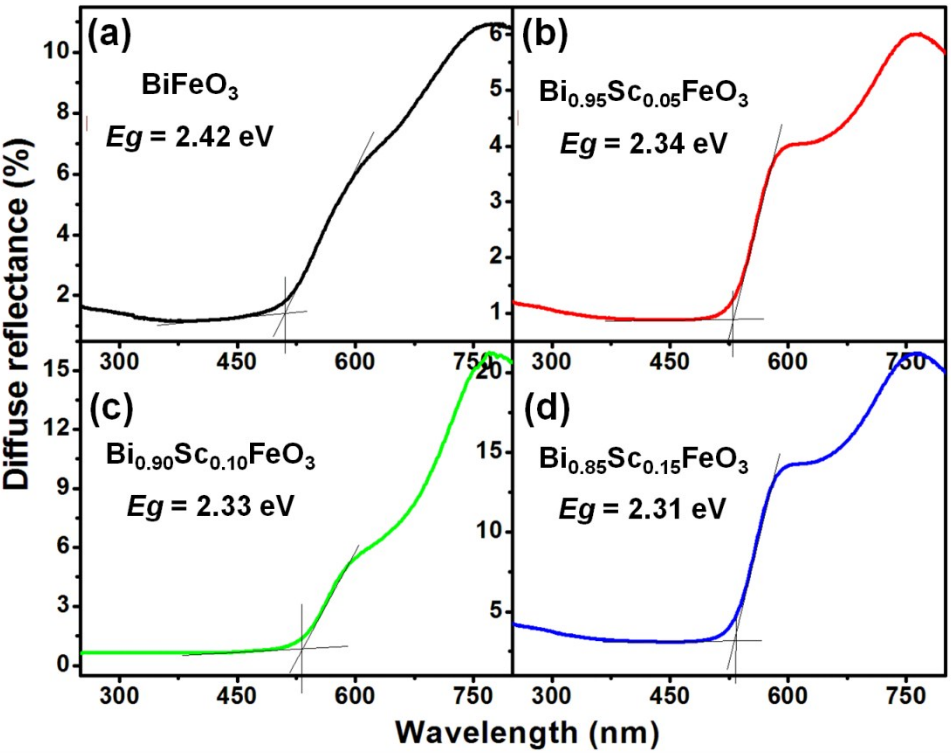

Fig. S6 Diffuse reflectance spectrum of $Bi_{1-x}Sc_xFeO_3$, fiber nanostructures, where x = (a) 0.0, (b) 0.05, (c) 0.10, and (d) 0.15.

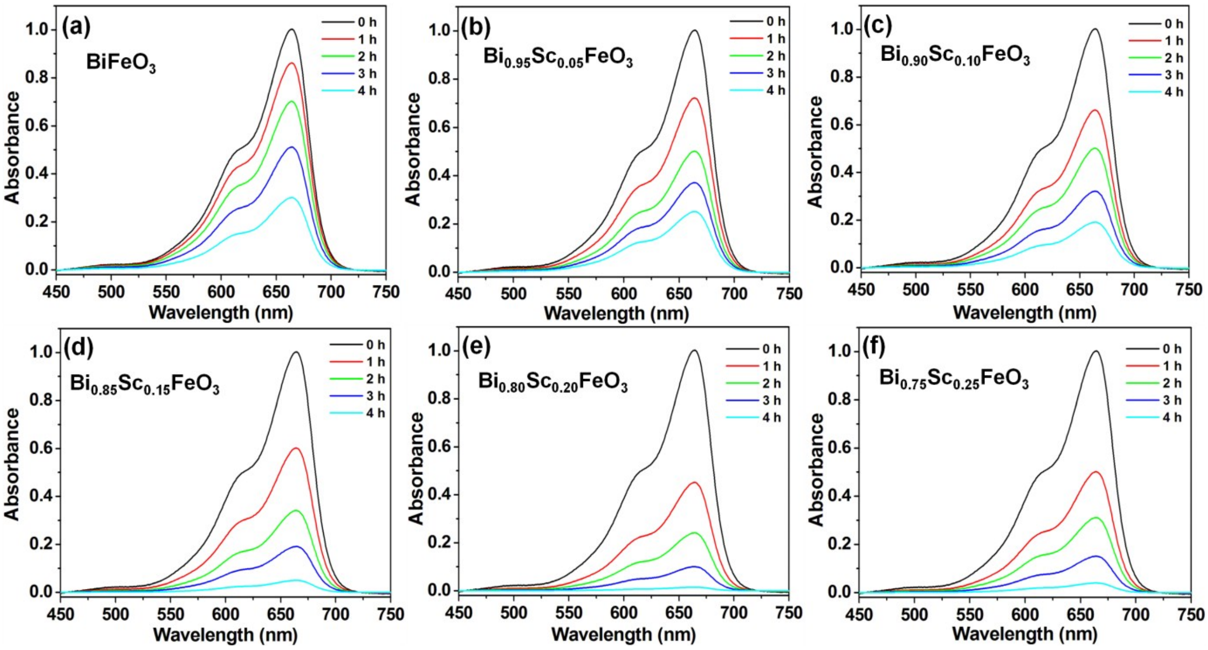

Fig. S7 (a)-(f) Photocatalytic degradation spectra of $Bi_{1-x}Sc_xFeO_3$ particulate nanostructures, where, x = (a) 0.0, (b) 0.05, (c) 0.10, (d) 0.15, (e) 0.20, and (f) 0.25.

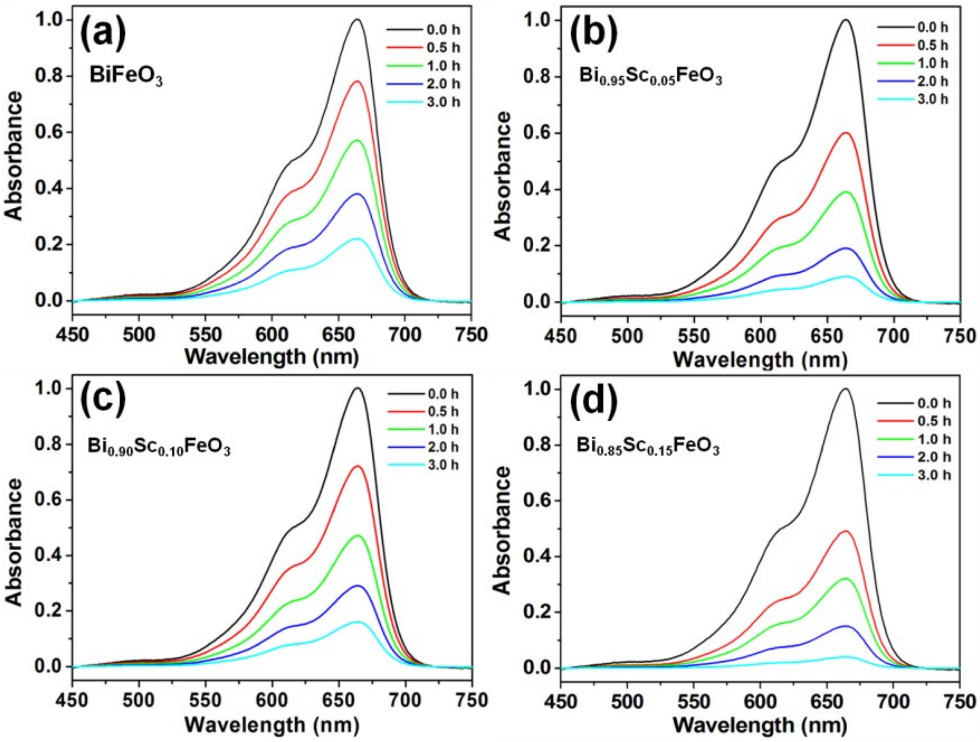

Fig. S8 (a)-(d) Photocatalytic degradation spectra of Bi$_{1-x}$Sc$_x$FeO$_3$ fiber nanostructures, where, x = (a) 0.0, (b) 0.05, (c) 0.10, and (d) 0.15.

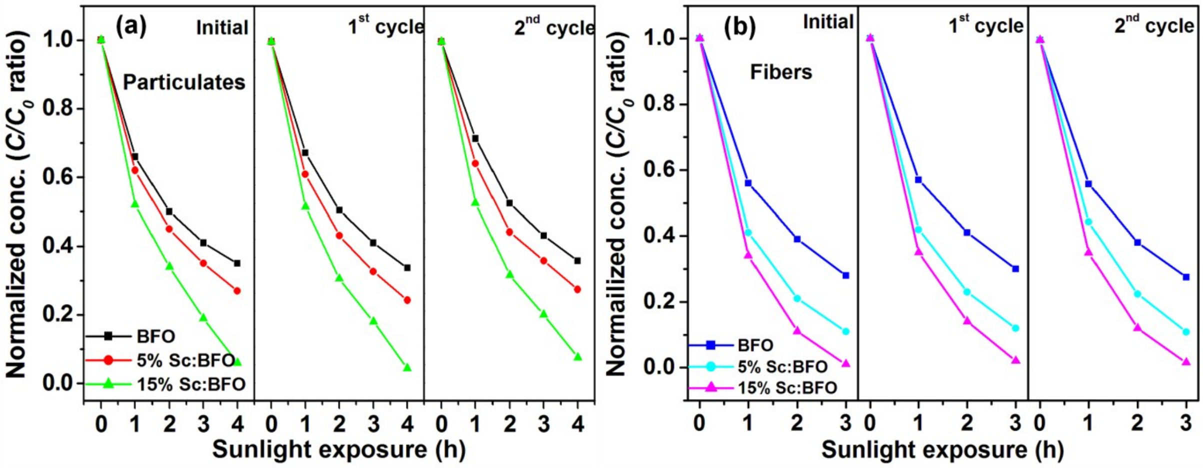

Fig. S9 Recyclability photocatalytic efficiency of (a) particulates and (b) fibers of pure BiFeO$_3$ and Bi$_{0.85}$Sc$_{0.15}$FeO$_3$ compositions.